Double-layer Perfect Metamaterial Absorber
and Its Application for RCS Reduction of Antenna

Sijia LI, Xiangyu CAO, Tao LIU, Huanhuan YANG

School of Information and Navigation, Air Force Engineering University, Street Feng Hao No.1, 710077 Xi'an, China

lsj051@126.com, xiangyucaokdy@163.com, lt9571@163.com, jianye8901@126.com

Abstract. *To reduce the radar cross section (RCS) of a circularly polarized (CP) tilted beam antenna, a double-layer perfect metamaterial absorber (DLPMA) in the microwave frequency is proposed. The DLPMA exhibits a wider band by reducing the distance between the three absorption peaks. Absorbing characteristics are analyzed and the experimental results demonstrate that the proposed absorber works well from 5.95 GHz to 6.86 GHz (relative bandwidth 14.1%) with the thickness of 0.5 mm. Then, the main part of perfect electric conductor ground plane of the CP tilted beam antenna is covered by the DLPMA. Simulated and experimental results reveal that the novel antenna performs well from 5.5 GHz to 7 GHz, and its monostatic RCS is reduced significantly from 5.8 GHz to 7 GHz. The agreement between measured and simulated data validates the present design.*

Keywords

RCS, perfect metamaterial absorber, tilted beam antenna, circular polarization.

1. Introduction

Nowadays, it has been a topic of immense strategic interest to reduce radar cross section (RCS) of an antenna without compromising its radiation characteristics. For out-of-band frequencies, it is well known that the RCS of antenna/array can be significantly reduced by placing a suitably shaped bandpass radome, such as frequency selective surfaces (FSS) in front of it [1]-[3]. However, when the radome is transparent, no significant RCS reduction of the antenna will take place for in-band frequencies. As an excellent candidate, the metamaterial absorber has been paid attention for in-band RCS reduction. In [4], to reduce the in-band RCS of ridged waveguide slot antenna array, the electromagnetic band-gap (EBG) loaded with lumped resistances has been investigated, in which the lumped resistive elements are used to better match to 377 Ω (the impedance of free space). A hybrid surface combined artificial magnetic conductor (AMC) with perfect electric conductor (PEC) for in-band RCS reduction of waveguide slot antenna has been reported in [5] based on the principle of passive cancellation. Then in [6], two different AMCs are analyzed for ultrathin and broadband radar absorbing material design. In [7], the reflection characteristics of a composite planar AMC surface has been investigated and fabricated for broadband RCS reduction. However, it is obvious that the RCS is reduced in boresight direction but increased in other directions. Recently, the perfect meta-material absorber with near-unity absorptivity has been investigated and has become an important aspect in the research of metamaterials in [8], [9]. In 2013, a perfect metamaterial absorber with polarization-insensitive and wide-angle absorption has been presented for RCS reduction of waveguide slot antenna in [10]. The maximum absorptivity of this absorber is 99.8% with a full-width at half-maximum (FWHM) of 220 MHz. However, the bandwidth is narrow for RCS reduction of broadband antenna.

In this paper, a bandwidth-enhanced double-layer perfect metamaterial absorber (DLPMA) is designed to reduce the RCS of a circularly polarized (CP) tilted beam broadband antenna. Three responses have been produced by the DLPMA, and the bandwidth is enhanced by reducing the distance between the three absorption peaks. The experimental results reveal that the proposed absorber exhibits a FWHM of 14.1% with the thickness of 0.5 mm. And then, its application on the in-band RCS reduction of broadband CP antenna has been investigated. The simulated and experimental results report that the DLPMA can absorb the incident wave effectively, and the monostatic RCS of the antenna is significantly reduced. Meanwhile, the gain of the proposed antenna is remained. The measured results show that the RCS reduction of the antenna is above 3 dB within the operation band from 5.5 GHz to 7 GHz and the most reduction values exceed 15.8 dBsm, 8.1dBsm, and 9.8 dBsm at the resonances.

2. Design and Analysis of DLPMA

As shown in Fig. 1, the proposed absorber is composed of three conductive layers with two substrates between them. Fig. 1(a) is the side view. Fig. 1(b) and 1(c) are the top view and the middle layer view. As the conductive layers, the copper (with the thickness of 18 μm and a conductivity of $\sigma = 5.8 \times 10^7$ S/m) is designed upon the lossy FR4 substrate along with dielectric constant (ε_r) of

4.4, length of a_6 and tangent of 0.02. On the top layer, a single-square loop with four splits in the four sides and a square metal patch in the center are designed on FR4 substrate with height of t_1. The loop copper (with inner-length of a_1 and the outer-length of a_2) and the metal patch (with length of a_3) both manipulate the electromagnetic resonance at different frequencies and increase the coupling losses, so that the transmitted wave can be reduced. a_4 is length of the four splits. On the second layer, a square metal patch with the length of a_5 is constructed on one side of FR4 substrate with height of t_2. The bottom layer is of a solid metal on the other side of the FR4 substrate. a_3 and a_5 for the two square metal patch depend on the resonance at two different frequencies. a_1, a_2, and a_4 manipulate the resonance at another frequency. The heights of t_1, t_2 and tangent depend on the absorption capability.
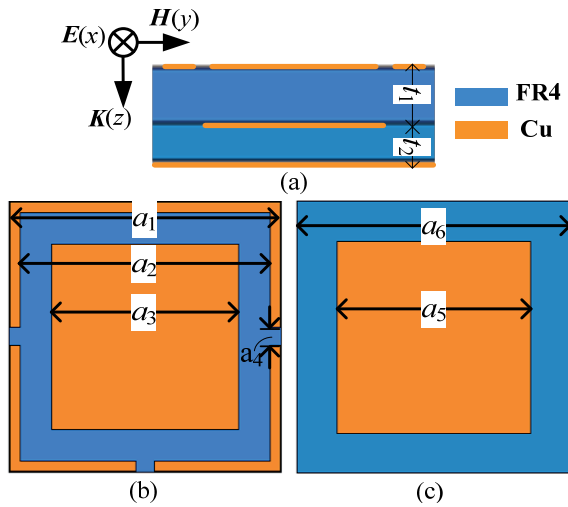
Fig. 1. Configuration of the DLPMA unit cell: (a) side view, (b) top view, (c) middle layer view.

We performed computer simulations of an ideal-but realizable-metamaterial absorber using the commercial finite element method (FEM) solver by ANSOFT HFSS 12.0. The absorptivity before optimization is shown in Fig. 2. The results reveal that the DLPMA doesn't display the great absorption capability and it is necessary to optimize the parameters of DLPMA. In order to enhance the bandwidth of DLPMA, the distance between the three absorption peaks has been reduced. The optimized geometries parameters are: $a_1 = 14.88$, $a_2 = 13.76$, $a_3 = 10.36$, $a_4 = 1$, $a_5 = 10.72$, $a_6 = 15$, $t_1 = 0.3$, $t_2 = 0.2$ (units: mm).

The optimized simulated absorptivity and the effective impedance for the structure are reported in Fig. 2. We can see that the three absorption peaks are respectively 99.6%, 78.2%, and 99.9% at 6.08 GHz, 6.42 GHz, and 6.76 GHz with a FWHM of 910 MHz (5.95 GHz to 6.86 GHz). In addition, we can find that the absorption peaks will obtain 100%, when the real part approaches to 377 Ω and the imaginary part approaches to zero. Owing to the high coupling losses from the single-square loop and the square metal patch, the double layer substrates can be reduced to 0.01λ ($t = t_1 + t_2 = 0.5$ mm).

Additionally, the simulated absorptivity as a function of frequency for the DLPMA is reported in Fig. 3 for TE and TM mode at various angles of incidence. Absorption peaks remain stable absorptivity with wide incident angles ranging from 0° to 60° for both TE and TM polarizations From Fig. 3, we conclude that the structure shows a wide-angle absorption and polarization-insensitive for TM mode and TE mode for all angles of incidence due to its symmetric structure in the XoY plane.
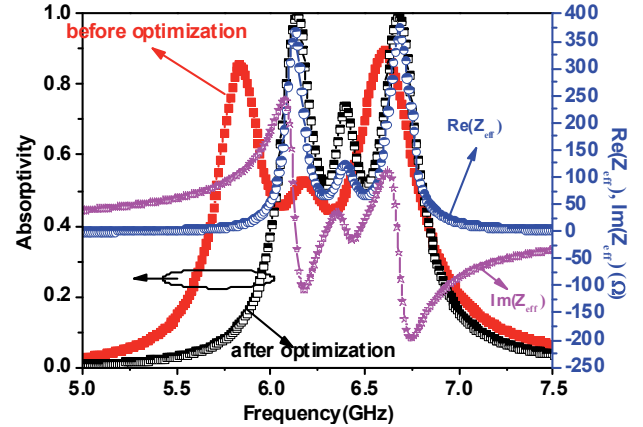
Fig. 2. Simulated absorptivity before & after optimization and the effective impedance of DLPMA cell.

The DLPMA displays a great absorption capability. The designed idea of the DLPMA is to adjust the effective $\varepsilon(\omega)$ and $\mu(\omega)$ independently by varying the dimensions of electric resonant component and magnetic resonant component in the unit cell so as to match the surface impedance to free space and achieve a large resonant dissipation at the meantime. And while, the tangent for the absorber is design for absorbing the microwave at the electric and magnetic resonants. Thus, the wave transmission and reflection are minimized simultaneously and absorption is maximized. As described in [8], [11], the absorptivity (A) is defined as

$$A = 1 - \left| S_{11} \right|^2 - \left| S_{21} \right|^2 = 1 - R - T . \quad (1)$$

R is the reflectivity, which is defined as $R = \left| S_{11} \right|^2$ and T is the transmission, whose definition is $T = \left| S_{21} \right|^2$. S_{11} and S_{21} are the S-parameters of the DLPMA. $T = 0$ because the bottom layer has a copper ground plate without patterning. Therefore, the absorptivity is defined as

$$A = 1 - \left| S_{11} \right|^2 = 1 - R . \quad (2)$$

The free-space reflection coefficient of DLPMA cell at normal incidence is given by [12], [13]

$$R = \frac{z_{eff}(\omega) - \eta_0}{z_{eff}(\omega) + \eta_0} \quad (3)$$

where η_0 represents the impedance of free space and is approximately 377 Ω. $z_{eff}(\omega)$ is the effective impedance of the DLPMA cell, which includes the surface impedance which is to achieve a large resonant dissipation and the

substrate impedance due to the high tangent. By substitution of (3) in (2), A can be written by

$$A = \frac{2\eta_0}{\text{Re}\left[z_{eff}(\omega)\right] + i \cdot \text{Im}\left[z_{eff}(\omega)\right] + \eta_0} \quad (4)$$

where $\text{Re}[z_{eff}(\omega)]$ and $\text{Im}[z_{eff}(\omega)]$ are respectively the real part and the imaginary part of $z_{eff}(\omega)$. When the DLPMA is at the resonant modes, the absorptivity $A = 1$. From the expression of (4), we know that when $A = 1$, $\text{Re}[z_{eff}(\omega)]$ and $\text{Im}[z_{eff}(\omega)]$ can be calculated as

$$\begin{cases} \text{Re}\left(z_{eff}(\omega)\right) = 377\Omega \\ \text{Im}\left(z_{eff}(\omega)\right) = 0 \end{cases} \quad (5)$$

It is found that the absorptivity of PMA is close to 100%, when the real part and imaginary part of the effective impedance are respectively close to 377 Ω and zero. The absorptivity is enhanced because of the different resonant modes.
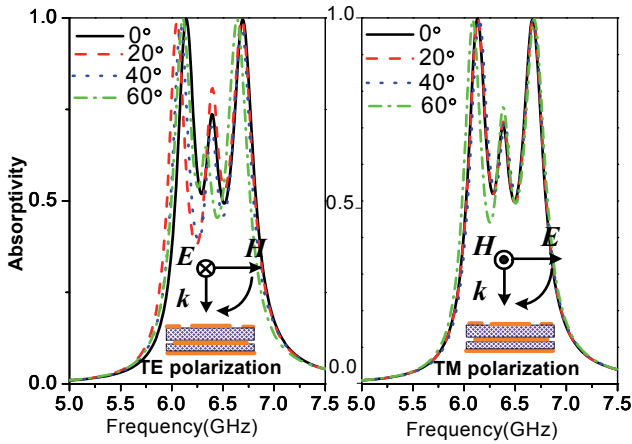
Fig. 3. Simulated absorptivity results of DLPMA at various angles of incidence for (a) TE and (b)TM mode.

3. RCS Reduction of CP Tilted Beam Antenna Using DLPMA

The antenna radiating titled beam has been widely used in many applications such as satellite communications, radars and global navigation satellite systems due to its advantages. The configurations of CP tilted beam antenna with the PEC and DLPMA ground planes are shown in Fig. 4. The antenna consists of a flower structure (FS), a helix feed line, a dielectric hollow cylinder, and a ground plane. The conventional antenna is loaded by PEC ground plane [14], [15]. Differently, the novel antenna is loaded by DLPMA and PEC ground plane. As shown in Fig. 4(a), the FS structure and helix feed line are printed on the dielectric (Taconic TLY, thickness is 1 mm, $\varepsilon_r = 2.2$, $\tan\delta = 9 \times 10^{-4}$) hollow cylinder, which has a radius(r) of 13.6 mm and a total height of 13.6 mm. The length (a) of the PEC ground plane is 120 mm 2.5λ (λ is the wavelength at 6.25 GHz). The thickness of the ground plane below the

dielectric hollow cylinder is 0.5 mm. The antenna is excited by a 50 Ω feed line. The FS structure is designed based on the single Archimedean spiral and its inner and outer equations are defined by

$$\begin{cases} r_{\text{in}} = r_1 + c_1\varphi + d_1 \dfrac{\varphi - \varphi_{\text{start}}}{\varphi_{\text{end}} - \varphi_{\text{start}}} \sin\left(n_1\varphi\right) \\ r_{\text{out}} = r_2 + c_2\varphi + d_2 \dfrac{\varphi - \varphi_{\text{start}}}{\varphi_{\text{end}} - \varphi_{\text{start}}} \sin\left(n_2\varphi\right) \end{cases} \quad (6)$$

where r_i is original radius of spiral line, c_i is the spiral constant, d_i and n_i are the amplitude and the angular frequency of the sine wave, respectively. $I = 1$ and 2 denote the inner and outer of the FS structure. $n_1 = n_2 = 40$. The optimized parameters are: $H = 13.6$, $D = 120$, $h_1 = 1.56$, $h_2 = 2.06$, $h_3 = 5.6$, $r_1 = 0.5$, $r_2 = 0.55$, $c_1 = 0.55$, $c_2 = 0.66$, $d_1 = d_2 = 0.5$(units: mm). Fig. 4(b) shows the novel tilted beam antenna which load three turns DLPMA in four sides of the small PEC ground plane. The whole ground size is the same size for one of conventional antenna. $d = 30$ mm.
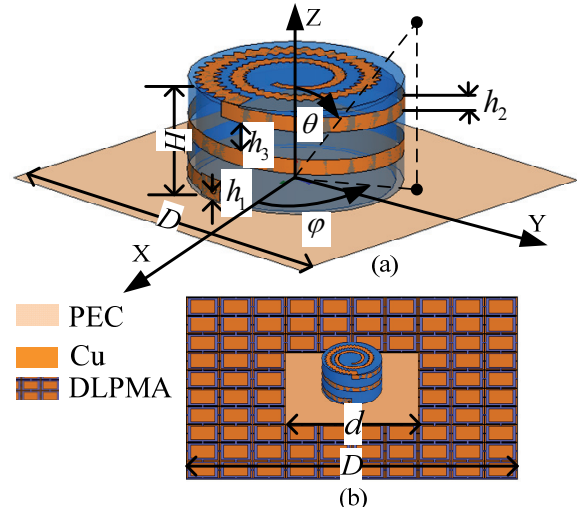
Fig. 4. Configuration of CP tilted beam antenna with (a) PEC ground plane, (b) DLPMA and small PEC ground plane. (novel antenna is CP tilted beam antenna with DLPMA and small PEC ground plane, conventional antenna is one with PEC ground plane).

The characters of the antenna radiation, (such as voltage standing wave ratio (VSWR), axial ratio (AR), and the radiation patterns) and scattering are simulated. The VSWR and AR results are shown in Fig. 5. The VSWR results are slightly shifted while the ground plane changed. The AR results of the novel and conventional antenna are hardly shifted. These indicate that the DLPMA and PEC ground plane negligibly affect the VSWR and AR for the antenna, when the feed location and the area of the ground plane are invariant. However, the AR will deteriorate as the ground plane reduces. So the large ground plane is necessary for the CP tilted beam antenna.

The radiation patterns of the antennas are reported in Fig. 6 at the 5.93 GHz and 6.74 GHz. From Fig. 6, we can see that the antenna patterns for both $\varphi = 0°$ and $\varphi = 90°$ have a very small variation for the different ground plates.

The gain remains steady due to the ground plane with same size (constructed of small PEC and DLPMA). The back lobe doesn't reduce because the surface wave below the antenna isn't suppressed by DLPMA. Thus the DLPMA ground plane is less sensitive to radiation characters.
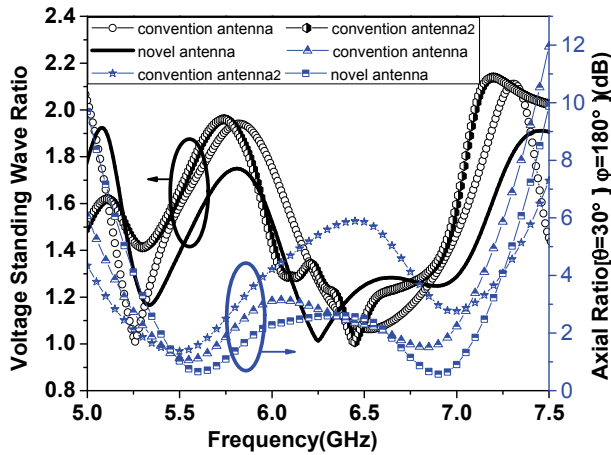
Fig. 5. Simulated VSWR and AR results of novel and conventional antennas (conventional antenna 2 is the antenna with PEC ground of *d*).

(a)

(b)
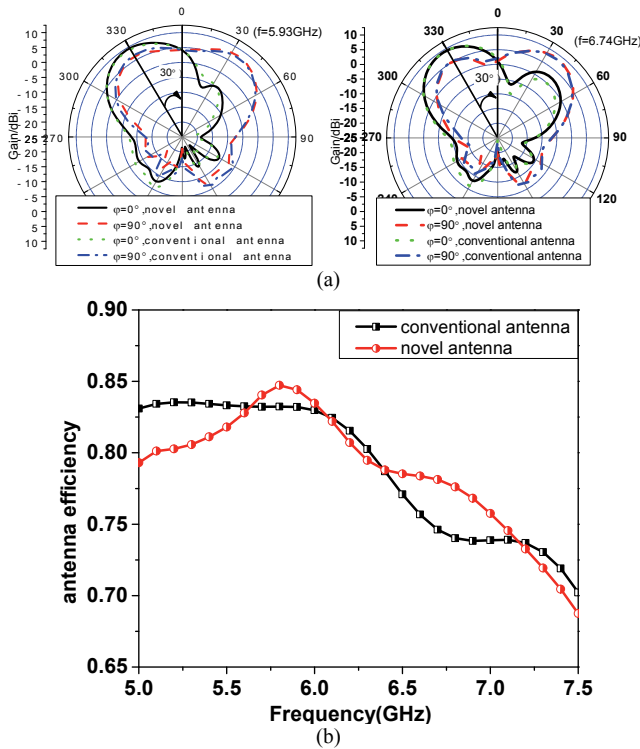
Fig. 6. (a).Simulated radiation patterns of the novel and conventional antennas at 5.93 GHz and 6.74 GHz. (b).Simulated antenna efficiency.

Fig. 7 gives the monostatic RCS results of novel and conventional antennas. We can see that there is the obvious in-band RCS reduction above 3 dBsm from 5.6 GHz to 6.9 GHz. The novel antenna has 16.6 dBsm, 8.5 dBsm, and 10.1 dBsm of RCS reduction peaks at 6.74 GHz, 6.34 GHz, and 5.93 GHz for TM polarization and 16.4 dBsm, 7.9 dBsm and 10.7 dBsm of ones at the same frequency

points for TE polarization. Note that there is frequency excursion between the RCS reduction peaks and the absorptivity peaks. It is because the periodic boundary conditions and Floquet port are utilized to simulate the infinite periodic cell, but DLPMA ground plane is finite.
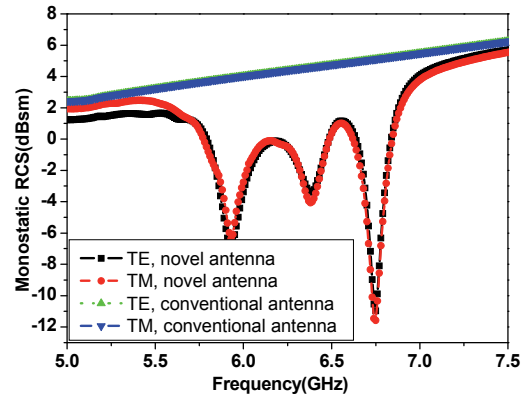
Fig. 7. Simulated monostatic RCS of novel and conventional antennas.

4. Fabrication and Measurement

The waveguide method [16], [17] was used for verifying the absorption in measurements. We connected the C-band standard waveguides (WR159, bandwidth is from 4.64 GHz -7.5 GHz) to a port of an Agilent N5230C network analyzer and mounted the sample into the port of the waveguide. The fabrication of the DLPMA (10×10 cells) is shown in Fig. 8. The parameters of DLPMA are kept the same with simulation. Fig. 9 gives the simulated and the measured absorptivity of the DLPMA. We can see that the three measured absorption peaks are respectively 98.2%, 76.5% and 99.1% at 6.02 GHz, 6.39 GHz and 6.73 GHz with a FWHM of 920 MHz(5.92 GHz-6.85 GHz), and simulated absorption peaks are 99.6%, 78.2% and 99.9% at 6.08 GHz, 6.42 GHz and 6.76 GHz with a FWHM of 910 MHz (5.95 GHz-6.86 GHz). In conclusion, the DLPMA have been verified by the good agreement between the simulation and experiment.
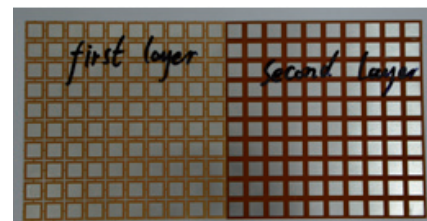
Fig. 8. Photograph of the practical DLPMA.

Fig. 10 presents the practical CP tilted beam antennas with different ground planes. The measured VSWR, AR and antenna efficiency results are reported in Fig. 11. As it is apparent, the novel antenna achieves an impedance bandwidth of approximately 36.1% at the center frequency of 6.1 GHz (5.0 GHz-7.2 GHz) and the measured AR bandwidth for the novel antenna is about 28.6%. As shown
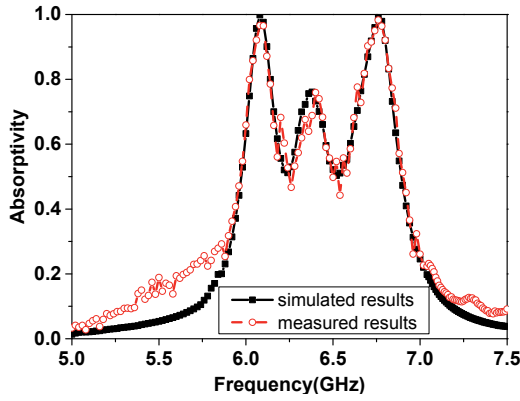
Fig. 9. Simulated and measured absorptivity of DLPMA.
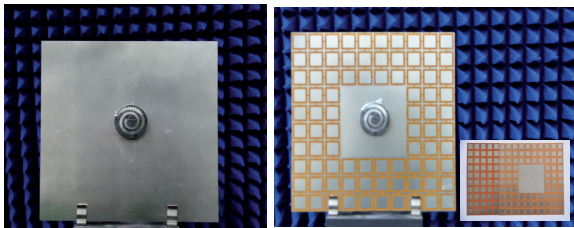
Fig. 10. Photograph of the conventional (left) and novel (right) practical antenna (Ground planes of antennas are same size).

(a)

(b)
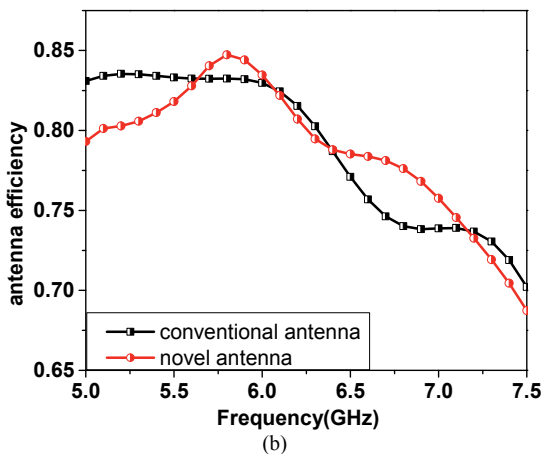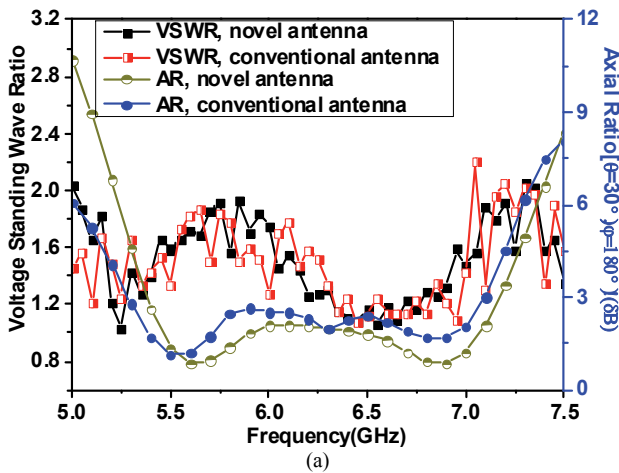
Fig. 11. (a) Measured VSWR and AR results of antennas; (b)measured antenna efficiency.

in Fig. 11(b), the novel and conventional antenna efficiencies are all obtained above 68% from 5 GHz to 7 GHz. The shift is neglectfully between the novel and conventional antenna efficiency. It can be summarized that the agreement of the simulated with the experimental results verifies the proposed antenna. And DLPMA slightly affects the radiation of the antenna.

The radiation patterns of the novel and conventional antennas with the same size ground plane were measured by Labvolt Antenna Measurement System and Anristu MG3692B Signal Generators in a microwave anechoic chamber. The measured radiation patterns with different ground planes are shown in Fig. 12 at 5.5 GHz, 6.0 GHz, 6.5 GHz, and 7 GHz. We can see that the beam azimuth angle is approximately 30° and the gain remains 8.5 dBi within the designed frequency range. The DLPMA ground plane does not remarkably affect the radiation pattern. Measured results demonstrate that the radiation characteristics of novel antenna are preserved basically. Summarily, theoretical and experimental results are in good agreement.
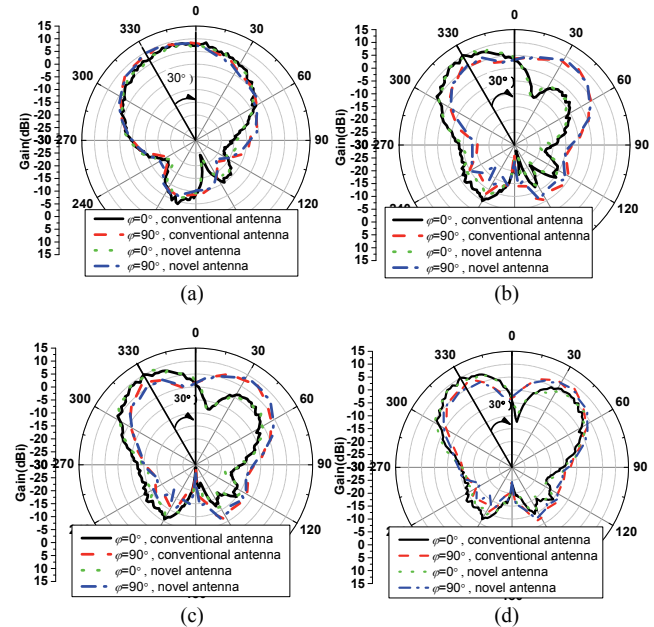
Fig. 12. Measured radiation patterns of novel and conventional antennas at (a) 5.5 GHz, (b) 6 GHz, (c) 6.5 GHz and (d) 7 GHz.

Two horn antennas method [18], [19] was used for antenna measurement and the monostatic RCS was measured from 5 GHz to 7.5 GHz. Two C-band horn antennas connected to a network analyzer were used, one for transmitting and the other for receiving. Fig. 13 gives the monostatic RCS of the novel and conventional antennas. As it is apparent, the novel antenna is characterized by a strong RCS reduction within the absorbing band of the DLPMA. We can see that there is evident RCS reduction above 3 dBsm from 5.8 GHz to 7 GHz. The peaks RCS in front direction have 15.8 dBsm, 8.1 dBsm and 9.8 dBsm (15.6 dBsm, 8 dBsm and 10.1 dBsm) reduction at 6.75 GHz, 6.35 GHz and 5.94 GHz for TM (TE) polarization.

It is worthwhile to point out that the most relevant RCS reduction for both TE and TM polarization occurs in correspondence of the frequency band where the DLPMA presents an absorptivity higher than 0.5. This simple design criterion has a great practical value since it illustrates the possibility to design the low-RCS CP tilted beam antenna.
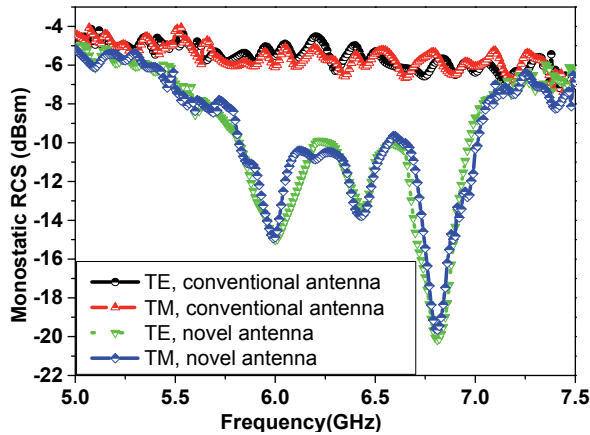
Fig. 13 Measured monostatic RCS of novel and conventional antennas for a normal incident TE and TM plane wave.

5. Conclusion

In this paper, a wideband-enhanced double-layer perfect metamaterial absorber has been introduced to reduce the in-band RCS of circularly polarization tilted beam antenna. By adjusting geometry parameters of the structure, we can obtain a polarization-insensitive and wide-incident-angle ultra-thin absorber whose absorption peaks are 98.2 %, 76.5 %, and 99.1 %. Its thickness is only 0.01λ and a full-width at half-maximum is 14.4 %. The experimental results show that the DLPMA can absorb the incident wave effectively, the monostatic RCS of the CP tilted beam antenna with the DLPMA is significantly reduced. Meanwhile, the radiation characters are remained. The measured results show that the antenna obtains the antenna efficiency of 68 % from 5 GHz to 7 GHz, an impedance bandwidth of approximately 36.1 % at the center frequency of 6.1 GHz and the measured AR bandwidth 28.6 %. Meanwhile, the RCS reduction of the antenna is above 3 dB within the operation band from 5.8 GHz to 7 GHz and the most reduction values exceed 15.8 dBsm, 8.1 dBsm and 9.8 dBsm at the resonances.

Acknowledgements

References

[1] GENOVESI, S., COSTA, F., MONORCHIO, A. Low profile array with reduced radar cross section by using frequency selective surfaces. *IEEE Transactions on Antennas Propagation*, 2012, vol. 60, no. 5, p. 2327-2335.

[2] ZHOU, H., QU, S.-B., LIN, B.-Q. Filter-antenna consisting of conical FSS radome and monopole antenna. *IEEE Transactions on Antennas Propagation*, 2012, vol. 60, no. 6, p. 3040-3045.

[3] WU, T. K. Improved dual band FSS performance with fractal elements. *Microwave and Optical Technology Letters*, 2012, vol. 54, no. 3, p. 833-835.

[4] LI, Y.-Q., ZHANG, H., FU, Y.-Q., YUAN, N.-C. RCS reduction of ridged waveguide slot antenna array using EBG radar absorbing material. *IEEE Antennas Wireless Propagation Letters*, 2008, vol. 7, p. 473-476.

[5] TAN, Y., YAN, N., YANG, Y., FU, Y. Improved RCS and efficient waveguide slot antenna. *Electronic Letters*, 2011, vol. 47, no. 10, p. 582-583.

[6] ZHANG, Y., MITTRA, R., WANG, B. Z, HUANG, N. T. AMCs for ultra-thin and broadband RAM design. *Electronic Letters*, 2009, vol. 45, no. 10, p. 484-485.

[7] HWANG, R. B., TSAI, Y. L. The reflection characteristics of a composite planar AMC surface. *AIP Advances*, 2012, no. 2, p. 012128.

[8] LANDY, N. I., SAJUYIGBE, S., MOCK, J. J., SMITH, D. R., PADILLA, W. J. A perfect metamaterial absorber. *Physical Review Letters*, 2008, vol. 100, p. 207402.

[9] VAN TUONG PHAM, PARK, J. W., DINH LAM VU, ZHANG, H. Y., RHEE, J. Y., KIM, K. W., LEE, Y. P. THz-metamaterial absorber. *Advanced. Nature Science: Nanoscience and Nanotechnology,* 2013, vol. 4, p. 015001.

[10] LIU, T., CAO, X.-Y., GAO, J., ZHENG, Q.-R., LI, W.-Q., YANG, H.-H. RCS reduction of waveguide slot antenna with metamaterial absorber. *IEEE Transactions on Antennas Propagation*, 2013, vol. 61, no. 4, p. 2327-2335.

[11] ZHU, B., WANG, Z., HUANG, C., FENG, Y., ZHAO, J., JIANG, T. Polarization insensitive metamaterial absorber with wide incident angle. *Progress in Electromagnetic Research*, 2010, vol. 10, no. 1, p. 231-239.

[12] SMITH, D. R., VIER, D. C., KOSCHNY, Th., SOUKOULIS, C. M. Electromagnetic parameter retrieval from inhomogeneous metamaterials. *Physical Review E*, 2005, vol. 71, p. 036617.

[13] LI, S.-J., CAO, X.-Y., GAO, J., ZHENG, Q.-R. Design of the ultra-thin perfect metamaterial absorber with high Q-factor. *Acta Physica Sinica,* 2013, vol. 62, no. 24, p. 244101.

[14] NAKANO, H., ASO, N., MIZOBE, N., YAMAUCHI, J. Low-profile composite helical-spiral antenna for a circularly-polarized tilted beam. *IEEE Transactions on Antennas Propagation*, 2011, vol. 59, no. 7, p. 2710-2713

[15] LI, S.-J., CAO, X.-Y., GAO, J., ZHENG, Q.-R., YANG, H.-H. Broadband and miniaturization of tilted beam antenna using CSRR splits and flower-spiral structure. *Microwave and Optical Technology Letters.* 2014, vol. 56, no. 1, p. 27-31.

[16] LI, L., YANG, Y., LIANG, C.-H. A wide-angle polarization-insensitive ultra-thin metamaterial absorber with three resonant modes. *Journal of Applied Physics,* 2011, vol. 110, p. 063702.

[17] SHANG, Y., XIAO, S., TANG, M.-C., BAI, Y.-Y., WANG, B. Radar cross-section reduction for a microstrip patch antenna using PIN diodes. *IET Microwave Antennas and Propagation*, 2012, vol. 6, no. 6, p. 670-679.

[18] LI, S.-J., CAO, X.-Y., GAO, J., ZHENG, Q.-R. Design of ultra-thin broadband metamaterial absorber and its application for RCS reduction of circular polarization tilted beam antenna. *Acta Physica Sinica,* 2013, vol. 62, no. 12, p. 124101.

About Authors ...

Sijia LI was born in Xi'an, Shaanxi province, P.R. China in 1987. He received B.Eng. degree from Guangxi University, Nanning, China, in June, 2009 and M. Eng. degree from the Telecommunication Engineering Institute, Air Force Engineering University of CPLA, Xi'an China, in 2011. Currently, he is working toward Ph.D degree at the School of Information and Navigation, Air Force Engineering University. His research activity has been focused in tilted beam antennas, perfect metamaterial absorber design and its application for antennas RCS reduction. He has authored and coauthored more than 30 technical journal articles and international conference papers.

Xiangyu CAO received the B.Sc and M.A.Sc degrees from Air Force the Missile Institute in 1986 and 1989, respectively. She joined the Air Force Missile Institute in 1989 as an assistant teacher. She became an associate professor in 1996. She received Ph.D. degree in the Missile Institute of Air Force Engineering University in 1999. From 1999 to 2002, she was engaged in postdoctoral research in Xidian University, China. She was a Senior Research Associate in the Department of Electronic Engineering, City University of Hong Kong from June 2002 to Dec 2003. She is currently a professor of the School of Information and Navigation, Air Force Engineering University of CPLA. She has authored and coauthored more than 120 technical journal articles and conference papers, and holds one China soft patent. Her research interests include computational electromagnetic, smart antennas, electromagnetic metamaterial and their antenna applications, and electromagnetic compatibility.

Tao LIU received the B.S., M.S., and Ph.D. degree from the Telecommunication Engineering Institute, Air Force Engineering University of CPLA, China, in 1999, 2005, and 2009, respectively. He is currently engaged in postdoctoral research at the same university. He has authored and coauthored more than 20 technical journal articles and conference papers. His research interest is in electromagnetic metamaterial and their antenna applications.

Huanhuan YANG received the B.S. and M.S. degree from the Telecommunication Engineering Institute, Air Force Engineering University of CPLA, China, in 2010, and 2012, respectively. Currently, he is working toward Ph.D degree at the School of Information and Navigation, Air Force Engineering University. His research interest is in electromagnetic metamaterial and their antenna applications. He has authored and coauthored more than 10 technical journal articles and international conference papers.